Singularity and Controllability Analysis of Parallel Manipulators and Closed-loop Mechanisms

Prasun Choudhury and Ashitava Ghosal[1]
Department of Mechanical Engineering,
Indian Institute of Science,
Bangalore — 560 012,
India.

Abstract

This paper presents a study of kinematic and force singularities in parallel manipulators and closed-loop mechanisms and their relationship to the controllability of such manipulators and closed-loop mechanisms. Parallel manipulators and closed-loop mechanisms are classified according to their degrees of freedom, number of output Cartesian variables used to describe their motion and the number of actuated joint inputs. The singularities in the workspace are obtained by considering the force transformation matrix which maps the forces and torques in joint space to output forces and torques in Cartesian space. The uncontrollable regions in the workspace are obtained by deriving the equations of motion in terms of Cartesian variables and by using techniques from Lie algebra. We show that when the number of actuated joint inputs is equal to the number of output Cartesian variables, and the force transformation matrix loses rank, the parallel manipulator is uncontrollable. For the case where the number of joint inputs is less than the number of output Cartesian variables, if the constraint forces and torques(represented by the Lagrange multipliers) become infinite, the force transformation matrix loses rank. Finally, we show that the singular and uncontrollable regions in the workspace of a parallel manipulator and closed-loop mechanism can be reduced by adding redundant joint actuators and links. The results are illustrated with the help of numerical examples where we plot the singular and uncontrollable regions of parallel manipulators and closed-loop mechanisms belonging to the above mentioned classes.

1 Introduction

Singularity, workspace and controllability of serial manipulators have been extensively studied and are very well understood(see for example [Sugimoto et. al., 1982, Wang and Waldron, 1987, Hunt, 1986, Lipkin and Pohl, 1991, Karger, 1996, Shamir, 1990]). In general, singularities of serial manipulators are characterized by the loss of one or more degrees of freedom and it has been shown that a serial manipulator will be uncontrollable at kinematic singularities where the velocity Jacobian loses rank. Several researchers have suggested control strategies to

[1]All correspondence with this author. Email: asitava@mecheng.iisc.ernet.in

avoid or pass through such singular configurations(see for example [Chang and Khatib, 1995, Tchnon and Matuszok, 1995, Chevallereau, 1996, Lloyd, 1996]). In the case of parallel manipulators and closed-loop mechanisms, singularity analysis is much more difficult since such mechanisms contain unactuated joints and joints with more than one degree of freedom. Singularities in parallel manipulators have been associated with either *loss or gain* of one or more degrees of freedom [Gosselin and Angeles, 1990]. In general, closed-form solutions for singular curves/surfaces for parallel manipulators of arbitrary architecture requires elimination of unwanted variables from several nonlinear transcendental equations, and this is quite difficult. Although some results are available for the singularities of planar and spatial parallel manipulators and closed-loop mechanisms(see for example the works of [Gosselin and Angeles, 1990, Sefrioui and Gosselin, 1995, Danielli et. al, 1995, Merlet, 1989, Hunt, 1978, Collins and Long, 1995, Basu and Ghosal, 1997, Zlatanov et. al., 1995, Fichter, 1986]), controllability of parallel manipulators has not been addressed adequately.

There exists general theories on controllability of non-linear systems(see for example the works of [Herman and Krenner, 1977, Isidori, 1995, Nijmeijer, 1990, Sussman and Jurdjevic, 1972]) and these results have been applied to systems with non-holonomic constraints and described by a set of differential-algebraic equations [Bloch and McClamroch, 1990, Sarkar et. al., 1994, Krishnan and McClamroch, 1994]. The equations of motion of parallel manipulators can be described by a set of differential-algebraic equations with holonomic constraint equations, and these have not been addressed adequately in literature. As far as the authors are aware, there exists no work, regarding the relationship between the singular and uncontrollable configurations in the workspace of parallel or hybrid manipulators and closed-loop mechanisms.

In this paper, we present theoretical and numerical results dealing with the relationship between the singular and uncontrollable regions in the workspace of parallel manipulators and closed-loop mechanisms when they *gain* one or more degrees of freedom. The parallel manipulators and closed-loop mechanisms are classified according to their degrees of freedom, the number of output Cartesian variables used to describe their motion and the number of actuated joint inputs. The singularities in the workspace of a parallel manipulator are studied by considering the force transformation matrix which maps the forces and torques in joint space to output forces and torques in Cartesian space. The uncontrollable regions in the workspace of the parallel manipulator are obtained by deriving the equations of motion in terms of Cartesian variables and by using techniques from Lie algebra. We show that when the number of joint inputs is equal to the number of output Cartesian variables, and the force transformation matrix loses rank, the parallel manipulator is uncontrollable. For the case of manipulators where the number of joint inputs is less than the number of output Cartesian variables, if the constraint forces and torques(represented by the Lagrange multipliers) become infinite the force transformation matrix loses rank. Finally, we show that the singular and uncontrollable regions

in the workspace of a parallel manipulator can be reduced by adding redundant joint actuators and links. The results are illustrated with the help of numerical examples where we plot the singular and uncontrollable regions of the above mentioned classes of parallel manipulators.

The paper is organized as follows: In section 2, we describe in brief the notion of a force transformation matrix and its relationship to the singularities of parallel manipulators. In section 3, we present the Lie algebra based method for controllability analysis of parallel manipulators and closed-loop mechanisms. In section 4, we present illustrative examples for various types of parallel manipulators and closed-loop mechanisms and in section 5, we present the conclusions.

2 Force Transformation Matrix and Singularity

The equations of motion of a parallel manipulator or a closed-loop mechanism, in terms of Cartesian variables $\mathbf{X}$[2], can be written as

$$\mathbf{M}(\mathbf{X})\ddot{\mathbf{X}} + \boldsymbol{\eta}(\mathbf{X}, \dot{\mathbf{X}}) = \mathbf{H}_s(\mathbf{X})\boldsymbol{\tau}_a + \mathbf{H}_k\boldsymbol{\lambda} \tag{1}$$

where $\mathbf{M}$ is the mass matrix, $\boldsymbol{\eta}$ is the vector containing the non-linear terms, $\boldsymbol{\tau}_a$ is the column vector of the actuator forces/torques and $\boldsymbol{\lambda}$'s are the constraint forces or the Lagrange multipliers. The matrix $\mathbf{H}$ given by

$$\mathbf{H} = \begin{bmatrix} \mathbf{H}_s & \mathbf{H}_k \end{bmatrix}$$

is called the *force transformation* matrix [Fichter, 1986]. The force transformation matrix, $\mathbf{H}$, maps the joint forces/torques, $\boldsymbol{\tau}$, to the output forces/torques on the end-effector in Cartesian space, $\mathbf{F}$, according to the relation

$$\mathbf{F} = \mathbf{H}\boldsymbol{\tau}.$$

In certain cases, the constraint equations can be eliminated and we can write the equations of motion as

$$\mathbf{M}(\mathbf{X})\ddot{\mathbf{X}} + \boldsymbol{\eta}(\mathbf{X}, \dot{\mathbf{X}}) = \mathbf{H}_s(\mathbf{X})\boldsymbol{\tau}_a \tag{2}$$

From equation 2, we see that the input forces/moments can be written as

$$\boldsymbol{\tau}_a = \mathbf{H}_s{}^{-1}(\mathbf{X})[\mathbf{M}(\mathbf{X})\ddot{\mathbf{X}} + \boldsymbol{\eta}(\mathbf{X}, \dot{\mathbf{X}})] \tag{3}$$

From the above equation, we observe that the actuator torques/forces will attain infinitely large values if the $\mathbf{H}$ matrix(same as $\mathbf{H}_s$ in this case) is rank deficient or the columns of the $\mathbf{H}_s$ matrix are linearly dependent. Hence, the rank deficiency of the $\mathbf{H}_s$ matrix leads to the condition of

[2]The Cartesian variables denote the position and orientation of an output link or the end-effector.

force singularities in the manipulators. At such singularities, the manipulator *gains* one or more degrees of freedom(see also [Hunt, 1978, Merlet, 1989]).

In case the constraint equations cannot be eliminated, in addition to the actuator forces/torques becoming infinite, the constraint forces given by the Lagrange multipliers can also go to infinity and we need to consider the rank deficiency of the matrix $\mathbf{H}_k$.

The columns of the force transformation matrix for manipulators with prismatic actuators are the Plücker coordinates [Hunt, 1978] of the joints of the mechanism, and are of the form

$$H_i = \begin{bmatrix} \mathbf{S}_i \\ \mathbf{q}_i \times \mathbf{S}_i \end{bmatrix} \tag{4}$$

where $\mathbf{S}_i$ is a vector along the joint axis and $\mathbf{q}_i \times \mathbf{S}_i$ is the moment of $\mathbf{S}_i$ with respect to a coordinate system. For manipulators with revolute actuators, the force transformation matrix can also be written in terms of the Plücker vectors, however, one has to choose the joint axis of the actuated joints and the moment term has to carefully evaluated with respect to the chosen coordinate system.

For a planar mechanism, the dimension of H_i is 3×1 and for a spatial mechanism the dimension is 6×1. In general for those manipulators and closed-loop mechanisms where the constraints can be totally eliminated, the force transformation matrix $\mathbf{H}$ has dimension $m \times n$ where n is the number of actuated joints and m is the number of task space coordinates(3 for planar mechanisms and 6 for spatial mechanisms).

3 Controllability Analysis

For the purpose of controllability studies of an n degree of freedom mechanical system, the nonlinear equations of motion are typically written as a set of $2n$ first order ordinary differential equations in terms of state variables. The state-space equations can, in general, be written as

$$\dot{\mathbf{x}} = \mathbf{f}(\mathbf{x}) + \sum_{i=1}^{m} \mathbf{g}_i(\mathbf{x})\mathbf{u}_i \tag{5}$$

where $\mathbf{x}$ is the vector of the state-variables, $\mathbf{f}$ and $\mathbf{g}$ represent the dynamics of the plant and the controller respectively, and u_i's are the m control inputs. We list a few definitions for the purpose of controllability analysis of systems modeled under the framework of equation (5).

- A control Lie algebra is the smallest sub-algebra, $\mathbf{C}$, containing the vector fields $\mathbf{f}$, $\mathbf{g}_1$, $\mathbf{g}_2$,..., $\mathbf{g}_m$ where $\mathbf{f}$ and $\mathbf{g}$ determine the dynamics of the plant and the controller (see equation (5)).

- A distribution Δ_c is the span $\Gamma \ : \ \Gamma \epsilon \mathbf{C}$, where $\Gamma = \mathbf{f} + \sum_{i=1}^{m} \mathbf{g}_i \mathbf{u}_i$ and Γ always remains in Δ_c.

A *sufficient* condition for a control system of the form given in equation (5) to be small time locally controllable(STLC) [Nijmeijer, 1990]at a point $(\mathbf{x}_0,\ \dot{\mathbf{x}}_0)$ is that $dim\Delta_c(\mathbf{x}_0, \dot{\mathbf{x}}_0) = n$ or $rank[\mathbf{C}] = n$. It may be noted that checking the rank of the distribution Δ_c is the same as checking the rank of the controllability matrix $\mathbf{C}$ because the matrix $\mathbf{C}$ is the smallest sub-algebra such that Γ spans the distribution Δ_c.

In non-redundant serial manipulators with n degrees of freedom, the $2n$ state variables are the n joint variables and the n joint velocities, and the number of actuated joints m is usually the same as n. In case of parallel manipulator and closed-loop mechanisms, there exists unactuated joints, and we can have the number of output variables, n, greater than, equal to or less than the number of actuated inputs, m. In addition, we can also have under-actuated systems where m is less than the degree of freedom(DOF) of the mechanism. We next evaluate the control algebra $\mathbf{C}$ for different forms of parallel manipulators and closed-loop mechanisms classified according to the the number of output variables(n), the number of input actuations(m) and the degree of freedom(DOF).

3.1 Manipulators with $m = n$

In parallel manipulators where the number of output Cartesian variables are the same as the number of actuated joint inputs, such as the well known Stewart Platform, by a suitable choice of Cartesian variables, the loop-closure (holonomic) constraint can be eliminated. In such cases, we can write the state equations as

$$\begin{pmatrix} \dot{\mathbf{x}}_1 \\ \dot{\mathbf{x}}_2 \end{pmatrix} = \begin{pmatrix} \mathbf{x}_2 \\ -\mathbf{M}^{-1}\boldsymbol{\eta} \end{pmatrix} + \begin{pmatrix} 0 \\ \mathbf{M}^{-1}\mathbf{H} \end{pmatrix} \boldsymbol{\tau} \tag{6}$$

where $\mathbf{x}_1$ and $\mathbf{x}_2$ denote the generalized co-ordinates (position/orientation variables) and their derivatives. Comparing with equation (5), we observe that

$$\mathbf{f} = \begin{pmatrix} \mathbf{x}_2 \\ -\mathbf{M}^{-1}\boldsymbol{\eta} \end{pmatrix}$$

and

$$\mathbf{g} = \begin{pmatrix} 0 \\ \mathbf{M}^{-1}\mathbf{H} \end{pmatrix}$$

For such manipulators, the control algebra is given by

$$\mathbf{C} = [\mathbf{g}_i, [\mathbf{f}, \mathbf{g}_i]]; \quad \forall i = 1, ...n \tag{7}$$

where $\mathbf{g}_i$ represents the i-th column of the $\mathbf{g}$ matrix, and $[\mathbf{f}, \mathbf{g}_i]$ is the Lie Bracket([Isidori, 1995]) of the vector fields $\mathbf{f}$ and $\mathbf{g}_i$.

For this class of parallel manipulators, the STLC requirement is not satisfied if

1. The matrix $\mathbf{H}$ is rank deficient. This can be easily seen from the fact that

$$\mathbf{g} = \begin{pmatrix} 0 \\ \mathbf{M}^{-1}\mathbf{H} \end{pmatrix}$$

   and the columns of $\mathbf{g}$ are linearly dependent if $\mathbf{H}$ loses rank.

2. If the vector fields $\mathbf{f}$ and $\mathbf{g}_i$'s are involutive, i.e., if any of the vectors $[\mathbf{f}, \mathbf{g}_i]$, $i = 1, ..., m$, can be expressed as a linear combination of vector fields $\mathbf{f}$ and $\mathbf{g}_i$'s.

3. If any of the columns of $[\mathbf{f}, \mathbf{g}_i]$ are linearly dependent on other columns of $[\mathbf{f}, \mathbf{g}_i]$.

For most parallel manipulators, it is extremely difficult to obtain closed form expressions for the above conditions, and in this paper, we have calculated the controllability conditions numerically(see section 4). However, from condition 1 in the above discussion we can conclude that force singularity is always a subset of the regions where the STLC condition is violated for parallel manipulators and closed-loop mechanisms with $m = n$.

In section 4, we present numerical results showing the singular configuration and regions where the STLC criteria is not satisfied.

3.2 Redundant Manipulators with $m > n$

To the basic structure of the Stewart Platform with six legs and six actuators if we add another leg with an actuated joint, then the number of degrees of freedom for the Stewart Platform still remains 6. However, in such a case, the number of actuated joints are more than n(n is 6 in this case). For manipulators with $m > n$, the controllability matrix is of the form $\mathbf{C} = [\mathbf{g}_i, [\mathbf{f}, \mathbf{g}_i]]$; $\forall i = 1, ...m$. The controllability matrix in this case is rectangular of dimension $(2n \times 2m)$ and the manipulator will be uncontrollable if the rank of $\mathbf{C}$ becomes less than $2n$. The force transformation matrix, $\mathbf{H}$, is of dimension $(m \times n)$.

The rank of a matrix is given by the maximum number of linearly independent columns. Hence, to check the rank deficiency condition of $\mathbf{H}$(i.e. $rank(\mathbf{H}) < n$), we need to check the rank deficiency of $m-n+1$ square matrices of dimension $(n \times n)$. The matrix $\mathbf{H}$ is rank deficient when each of the individual square sub-matrices are rank deficient, since otherwise there will be n independent columns in the $\mathbf{H}$ matrix. This reasoning implies that the singularity manifold will be the intersection of the manifolds obtained by considering the rank deficiency of each of the $m-n+1$ square matrices([Dasgupta and Mruthyunjaya, 1998]). If the rank deficiency condition of each of the square matrices give surfaces, then the intersection will be along curves or points. Hence, it is expected that the complete singularity manifold will be smaller for a redundant

manipulator[3]. The region where the manipulator does not satisfy the STLC condition, by a similar reasoning, is expected to be smaller for a redundant parallel manipulator.

In section 4, we present numerical results for a redundant planar manipulator which illustrates the above reasoning.

3.3 Manipulators with $m < n$

In many parallel manipulators, it is not possible to eliminate the constraints and the equations of motion contain Lagrange multipliers[4]. In such cases, we adopt a normalization strategy used by Krishnan and McClamroch [Krishnan and McClamroch, 1994]. Using the transformations used by Krishnan and McClamroch, we can obtain a new set of state space equations given as

$$\begin{aligned} \dot{\overline{\mathbf{x}_1}} &= \overline{\mathbf{x}_2} \\ \dot{\overline{\mathbf{x}_2}} &= \dot{\mathbf{P}}(\mathbf{q})\dot{\mathbf{q}} - \mathbf{P}\mathbf{M}^{-1}(\mathbf{q})[\boldsymbol{\eta}(\mathbf{q},\dot{\mathbf{q}}) - \\ &\quad \mathbf{J}^T \times (\mathbf{J}\mathbf{M}^{-1}(\mathbf{q})\mathbf{J}^T)^{-1} \times [\mathbf{J}\mathbf{M}^{-1}(q)\boldsymbol{\eta}(\mathbf{q},\dot{\mathbf{q}}) - \dot{\mathbf{J}}(\mathbf{q})\dot{\mathbf{q}}] \\ &\quad + \mathbf{P}\mathbf{M}^{-1}(\mathbf{q})[\mathbf{E}_n - \mathbf{J}^T(\mathbf{J}\mathbf{M}^{-1}(\mathbf{q})\mathbf{J}^T)^{-1} \times \mathbf{J}\mathbf{M}^{-1}(\mathbf{q})]\mathbf{u} \end{aligned} \tag{8}$$

where $\mathbf{P}$ is given by

$$(\partial \mathbf{h}_1/\partial \mathbf{q})\dot{\mathbf{q}} = \mathbf{P}(\mathbf{q})\dot{\mathbf{q}}$$

and $\mathbf{h}_1$ are the output variables which have been chosen to be controlled and are equal in number to the degree of freedom of the system. The matrix $\mathbf{J}$ denotes the Jacobian of the constraints inherent to the system.

It may be noted that the input $\mathbf{u}$ in equation (8) when expressed in joint space is $\boldsymbol{\tau}$ and will be $\mathbf{H}_s\boldsymbol{\tau}$ when the equations of motion are expressed in task space. It can also be seen that the choice of output variables $\overline{\mathbf{x}_1}$ depends on the variables which are to be controlled, and hence the controllability characteristics will depend on the choice of the output co-ordinates.

The singularity matrix $\mathbf{H}$ will be rank deficient when either of the sub-matrices $\mathbf{H}_s$ or $\mathbf{H}_k$ will be rank deficient. The $\mathbf{H}_s$ matrix will be rank deficient if the matrix $\mathbf{H}_s$ of size 6×3 has rank less than 3.

From the expression of $\mathbf{g}$ it is clear that the rank deficiency of $\mathbf{H}_s$ will lead to linear dependency of the column vectors $\mathbf{g}_i$ and in turn the matrix $\mathbf{C}$ will be rank deficient. Hence, if $\mathbf{H}_s$ is rank deficient, the system will not be STLC.

[3]This reasoning has been used to show that in a Stewart Platform with an extra actuated leg, the singularities lie at most on a 16−th order geometric entity which may be solid, surface or curve(for a fixed orientation of the output platform) instead of on a quartic hyper-surface for the regular Stewart Platform.

[4]The 3-DOF spatial manipulator(see figure 3) falls under this category. In this case three Cartesian coordinates and three orientation variables are required to describe the motion of the top platform. However, since the mechanism has three degrees of freedom, the six coordinates are related to each other by three complex non-linear equations(see also section 4).

To see the effect of rank deficiency of $\mathbf{H}_k$, we rewrite equation(1) as

$$\boldsymbol{\lambda} = \mathbf{H}_k{}^{+}(\mathbf{X})\{\mathbf{M}(\mathbf{X})\ddot{\mathbf{X}} + \boldsymbol{\eta}(\mathbf{X}, \dot{\mathbf{X}}) - \mathbf{H}_s(\mathbf{X})\boldsymbol{\tau}\} + (\mathbf{I} - \mathbf{H}_k{}^{+}\mathbf{H}_k)\boldsymbol{\nu} \tag{9}$$

where $\mathbf{H}_k{}^{+}$ is the pseudo-inverse of the matrix $\mathbf{H}_k$ given by $\mathbf{H}_k{}^{T}(\mathbf{H}_k\mathbf{H}_k{}^{T})^{-1}$ and $\boldsymbol{\nu}$ is any generalized vector such that $(\mathbf{I} - \mathbf{H}_k{}^{+}\mathbf{H}_k)\boldsymbol{\nu}$ lies in the null space of $\mathbf{H}_k$. From this equation we can see that if $\mathbf{H}_k$ loses rank, then it's pseudo-inverse $\mathbf{H}_k{}^{+}$ doesn't exist or in other words the Lagrange multipliers $\boldsymbol{\lambda}$ becomes infinite. Hence, if matrix $\mathbf{H}_k$, of dimension 6×3, has rank less than 3, the constraint forces become infinite.

Other than the loss of rank of $\mathbf{H}_s$ and $\mathbf{H}_k$, the matrix $\mathbf{H}$ can also become singular if the individual columns of $\mathbf{H}_s$ and $\mathbf{H}_k$ are linearly dependent amongst themselves. This signifies that the manipulator will be unable to withstand external load under certain combination of constraint and input forces.

In section 4, we present numerical results showing the singular configuration and regions where the STLC criteria is not satisfied for a spatial three-degree-of-freedom parallel manipulator.

3.4 Under-actuated manipulators with $m < DOF$

For a manipulator where the number of control inputs(m) is less than the degree of freedom(DOF), the control Lie algebra becomes more complicated. In such cases, we have to evaluate the Lie brackets of higher order. In equation (1) if $x \epsilon R^3$ and we have 2 control inputs(i.e. $m = 2$), then the controllability matrix $\mathbf{C}$ will contain the following columns:

$$\mathbf{C} = [\mathbf{g}_1, \mathbf{g}_2, [\mathbf{f}, \mathbf{g}_1], [\mathbf{f}, \mathbf{g}_2], [\mathbf{g}_1[\mathbf{f}, \mathbf{g}_2]], [\mathbf{f}[\mathbf{g}_1[\mathbf{f}, \mathbf{g}_2]]]] \tag{10}$$

In the above case the force transformation matrix, $\mathbf{H}$, will contain just 2 columns and the system will be under singular configuration when the $\mathbf{H}$ matrix of size 3×2 becomes rank deficient(i.e. $rank(\mathbf{H}) < 2$).

In section 4, we present numerical results for a planar closed-loop mechanism, showing the singular configurations and regions where the STLC criteria is not satisfied.

4 Results with Illustrative Examples

In this section we illustrate our theory through examples of parallel manipulators belonging to the four different cases discussed in the previous section. Since the expressions for $\det(\mathbf{H}) = 0$ and $\det(\mathbf{C}) = 0$ are very complicated in many cases, it is difficult to obtain any closed-form analytical results. In this section, we present plots of singular and uncontrollable regions obtained numerically based on the rank deficiency of $\mathbf{H}$ and $\mathbf{C}$ matrices. The numerical values

used for obtaining the plots are given in Appendix 1. The closed-form dynamic equations of motion for the respective manipulators have been obtained with the help of Newton-Euler formulation([Choudhury, 1997]). All the numerical results were obtained by using the software package Matlab.

4.1 Parallel Manipulator with $m = n$

The three-degree-of-freedom planar parallel manipulator, shown in figure 1, has three prismatic actuated joints and six passive revolute joints. The equations of motion of this planar manipulator are given by

$$\mathbf{M} \begin{bmatrix} \ddot{\mathbf{t}} \\ \alpha \end{bmatrix} + \boldsymbol{\eta} = \mathbf{H}\mathbf{f} \tag{11}$$

where the block elements of the mass matrix $\mathbf{M}$ are

$$\begin{aligned}
\mathbf{M}_{11} &= M_p\mathbf{E}_2 + \sum_{i=}^{3} \mathbf{Q}_i \\
\mathbf{M}_{12} &= {\mathbf{M}_{21}}^T = -(M_p\mathbf{R}_\perp + \sum_{i=1}^{3} \mathbf{Q}_i\mathbf{q}_{i\perp}) \\
\mathbf{M}_{22} &= I_p + M_p(R^2\mathbf{E}_2 - \mathbf{R}\mathbf{R}^T) + \sum_{i=1}^{3} \mathbf{q}_i^T{}_\perp \mathbf{Q}_i\mathbf{q}_{i\perp}
\end{aligned}$$

and

$$\begin{aligned}
\boldsymbol{\eta} &= \begin{bmatrix} M_p\{-\omega^2\mathbf{R} - \mathbf{g}\} + \sum_{i=1}^{3} \mathbf{U}_i \\ -M_p\mathbf{R} \times \mathbf{g} + \sum_{i=1}^{3} \mathbf{q}_i \times \mathbf{U}_i \end{bmatrix} \\
\mathbf{H} &= \begin{bmatrix} \mathbf{s}_1 & \mathbf{s}_2 & \mathbf{s}_3 \\ \mathbf{q}_1 \times \mathbf{s}_1 & \mathbf{q}_2 \times \mathbf{s}_2 & \mathbf{q}_3 \times \mathbf{s}_3 \end{bmatrix} \\
\mathbf{f} &= \begin{bmatrix} f_1 & f_2 & f_3 \end{bmatrix}^T
\end{aligned}$$

In the above equation, $\boldsymbol{\eta}$ is the column vector containing the centripetal, Coriolis and other non-linear terms, $\mathbf{H}$ is the force transformation matrix and vector $\mathbf{f}$ denote the input actuations. The terms a_1, $\mathbf{Q}$ and $\mathbf{U}$ are given as

$$\begin{aligned}
&a_1 = m_d{\mathbf{r}_{d\perp}}^2 + m_u{\mathbf{r}_{u\perp}}^2 + (I_u + I_d) \\
&\mathbf{Q} = m_u\mathbf{s}\mathbf{s}^T + \tfrac{a_1}{L^2}\mathbf{s}_\perp{\mathbf{s}_\perp}^T + \tfrac{m_u(\mathbf{r}_u \times \mathbf{s})}{L}(\mathbf{s}{\mathbf{s}_\perp}^T + \mathbf{s}_\perp\mathbf{s}^T) \\
&\mathbf{U} = [m_u\mathbf{s} \cdot \mathbf{g} + m_uW^2\mathbf{s} \cdot \mathbf{r}_u - m_uW^2\mathbf{s} \cdot L + 2m_uW\dot{L}\mathbf{s} \cdot \mathbf{r}_{u\perp}]\mathbf{s} \\
&+[m_u\mathbf{r}_u \times \mathbf{g} + m_d\mathbf{r}_d \times \mathbf{g} - 2m_u\dot{L}W\mathbf{r}_u \times \mathbf{r}_{u\perp} - m_uW^2L(\mathbf{r}_u \times \mathbf{s}) + 2(I_u + I_d)W\dot{L}]\mathbf{s}_\perp
\end{aligned}$$

where W is the angular velocity of the leg, $\perp$ denotes a positive rotation by a right-angle, $\mathbf{s}$ is the unit vector along the leg direction, $\dot{L}$ is the velocity of the leg with prismatic actuation, $\mathbf{R}$ denotes the centre of gravity of the platform in a reference frame about a base point and parallel

to the global frame, ω is the angular velocity of the platform, $\mathbf{q} = \Re\, \mathbf{p}$($\mathbf{p}$ denotes the platform point in local frame and $\Re$ is the rotation matrix which gives the orientation of the output platform), $\mathbf{r}_d$ and $\mathbf{r}_u$ denote the centre of gravity of upper and lower parts of the leg(in global frame), m_d and m_u denote the mass of lower and upper part of each leg, M_p denotes the mass of the platform, $\mathbf{I}_u$ and $\mathbf{I}_d$ are the inertia matrices of the upper and lower parts respectively $\mathbf{I}_p$ is the inertia matrix of the platform(in global frame) and $\mathbf{E}_2$ is a 2×2 identity matrix.

From the $\mathbf{H}$ matrix we can say that the mechanism does not have any kinematic singularity, though the manipulator is constrained due to the joint limits. Numerical simulations for the above manipulator were done with the parameters given in Appendix 1. The simulations were done for several constant orientations of the output platform and the workspace boundary was calculated based on the joint limits of all the prismatic joints. Sefroui and Gosselin [Sefrioui and Gosselin, 1995] have shown that the singularity curves will be quadratic in nature for a constant orientation of the output platform and similar conclusions can be inferred from the numerical results(see figure 5). From a geometric viewpoint the matrix $\mathbf{H}$ will be singular when the joint axes are either parallel or concurrent. The singular curves along with the workspace boundary for this manipulator are shown in the left column of figure 5.

The controllability matrix for this manipulator has dimension 6×6. The regions where the STLC condition is violated are shown on the right hand side of figure 5 along with the workspace boundary. It can be seen that the nature of the singular and uncontrollable regions are the same i.e. uncontrollability occurs around a singularity curve.

4.2 Hybrid manipulators

The 6-dof 3-PRPS hybrid manipulator shown in figure 4 has two prismatic actuations in each leg [Behi, 1988]. The equations of motion are given by:

$$\mathbf{M} \begin{bmatrix} \ddot{\mathbf{t}} \\ \boldsymbol{\alpha} \end{bmatrix} + \boldsymbol{\eta} = \mathbf{H}\mathbf{F} \tag{12}$$

where

$$\begin{aligned}
\mathbf{M} &= \begin{bmatrix} M_p\mathbf{E}_3 + \sum_{i=}^{3} \mathbf{Q}_i & -(M_p\widetilde{\mathbf{R}} + \sum_{i=1}^{3} \mathbf{Q}_i\widetilde{\mathbf{q}}_i) \\ M_p\widetilde{\mathbf{R}} + \sum_{i=1}^{3} \widetilde{\mathbf{q}}_i\mathbf{Q}_i & \mathbf{I}_p + M_p(\mathbf{R}^2\mathbf{E}_3 - \mathbf{R}\mathbf{R}^T) + \sum_{i=1}^{3} \widetilde{\mathbf{q}}_i\mathbf{Q}_i\widetilde{\mathbf{q}}_i \end{bmatrix} \\
\boldsymbol{\eta} &= \begin{bmatrix} M_p\{\boldsymbol{\omega} \times (\boldsymbol{\omega} \times \mathbf{R}) - \mathbf{g}\} + \sum_{i=1}^{3} \mathbf{U}_i \\ \boldsymbol{\omega} \times (\mathbf{I}_p\boldsymbol{\omega}) + M_p\mathbf{R} \times \{(\boldsymbol{\omega} \cdot \mathbf{R})\boldsymbol{\omega} - \mathbf{g}\} + \sum_{i=1}^{3} \mathbf{q}_i \times \mathbf{U}_i \end{bmatrix} \\
\mathbf{H} &= \begin{bmatrix} \mathbf{k}_1 & \mathbf{k}_2 & \mathbf{k}_3 & \mathbf{s}_1 & \mathbf{s}_2 & \mathbf{s}_3 \\ \mathbf{q}_1 \times \mathbf{k}_1 & \mathbf{q}_2 \times \mathbf{k}_2 & \mathbf{q}_3 \times \mathbf{k}_3 & \mathbf{q}_1 \times \mathbf{s}_1 & \mathbf{q}_2 \times \mathbf{s}_2 & \mathbf{q}_3 \times \mathbf{s}_3 \end{bmatrix} \\
\mathbf{F} &= \begin{bmatrix} f_{k_1} & f_{k_2} & f_{k_3} & f_{s_1} & f_{s_2} & f_{s_3} \end{bmatrix}^T
\end{aligned}$$

As described earlier, $\mathbf{M}$ is the mass matrix, $\boldsymbol{\eta}$ contains all the centripetal and Coriolis terms, matrix $\mathbf{H}$ is the force transformation matrix, $\mathbf{F}$ denote the vector of input actuations. The expressions for $\mathbf{Q}$ and $\mathbf{U}$ are given by

$$\begin{aligned}
\mathbf{Q} &= m_u \mathbf{s}\mathbf{s}^T + \frac{m_u}{L}\{\mathbf{s}\cdot(\mathbf{k}\times\mathbf{r}_u)\}\{\mathbf{s}(\mathbf{k}\times\mathbf{s})^T + (\mathbf{k}\times\mathbf{s})\mathbf{s}^T\} + (m_u+m_m+m_d)\mathbf{k}\mathbf{k}^T + a_1(\mathbf{k}\times\mathbf{s})(\mathbf{k}\times\mathbf{s})^T \\
\mathbf{U} &= [m_u(\mathbf{s}\cdot\mathbf{g}) - m_u\mathbf{s}\cdot\mathbf{W}\times(\mathbf{W}\times\mathbf{r}_u) - m_u u_3 - \frac{m_u}{L}\{\mathbf{s}\cdot(\mathbf{k}\times\mathbf{r}_u)\}u_4]\mathbf{s} \\
&\quad + [(m_u+m_m+m_d)(\mathbf{k}\cdot\mathbf{g}) - \{m_u\mathbf{W}\times(\mathbf{W}\times\mathbf{r}_u) + m_m\mathbf{W}\times(\mathbf{W}\times\mathbf{r}_m) \\
&\quad + m_d\mathbf{W}\times(\mathbf{W}\times\mathbf{r}_d)\}\cdot\mathbf{k} - 2m_u\dot{L}\mathbf{k}\cdot(\mathbf{W}\times\mathbf{s}) - (m_u+m_m)u_1 - m_u(\mathbf{k}\cdot\mathbf{s})u_3]\mathbf{k} \\
&\quad + [m_u\mathbf{k}\cdot(\mathbf{r}_u\times\mathbf{g}) + m_m\mathbf{k}\cdot(\mathbf{r}_m\times\mathbf{g}) - \mathbf{k}\cdot\{\mathbf{W}\times(\mathbf{I}_u+\mathbf{I}_m)\mathbf{W}\} - a_1u_4 - m_u\mathbf{k}\cdot(\mathbf{r}_u\times\mathbf{s})u_3](\mathbf{k}\times\mathbf{s})
\end{aligned}$$

where

$$a_1 = m_m(\mathbf{k}\times\mathbf{r}_m)^2 + m_u(\mathbf{k}\times\mathbf{r}_u)^2 + \mathbf{k}\cdot(\mathbf{I}_u+\mathbf{I}_m)\mathbf{k} \tag{13}$$

and

$$u_1 = \omega\times(\omega\times\mathbf{q}); \qquad u_2 = \mathbf{k}\cdot\mathbf{u}_1; \qquad u_3 = \mathbf{s}\cdot\mathbf{u}_1 + L\|\mathbf{W}\|^2; \qquad u_4 = \frac{\mathbf{k}\times\mathbf{s}}{L}\cdot\mathbf{u}_1 - 2\frac{\|\mathbf{W}\|\dot{L}}{L}$$

In the above expressions, $\mathbf{r}_m$ denote the centre of gravity of middle leg(in global frame) and m_m and $\mathbf{I}_m$ are the mass and the inertia matrix(in global frame) of the middle leg respectively. The directions of the prismatic joints at the base is given by the vector $\mathbf{k}$. All other notations are similar to the ones discussed earlier.

From the $\mathbf{H}$ matrix it is evident that the mechanism does not contain any kinematic singularity, though it is constrained to move in one direction(when the prismatic joint reaches it's limit). Numerical simulations of the above manipulator were done based on the parameters given in Appendix 1. It may be noted that the simulations are done for constant orientation of the the output platform.

The force transformation matrix, $\mathbf{H}$, can be written as:

$$\mathbf{H} = \begin{bmatrix} \mathbf{k}_1 & \mathbf{k}_2 & \mathbf{k}_3 & \mathbf{s}_1 & \mathbf{s}_2 & \mathbf{s}_3 \\ \mathbf{b}_1\times\mathbf{k}_1 & \mathbf{b}_2\times\mathbf{k}_2 & \mathbf{b}_3\times\mathbf{k}_3 & \mathbf{b}_1\times\mathbf{s}_1 & \mathbf{b}_2\times\mathbf{s}_2 & \mathbf{b}_3\times\mathbf{s}_3 \end{bmatrix}$$

The above can be further simplified to yield[5]:

$$\mathbf{H} \sim \begin{bmatrix} \mathbf{t}+\Re\mathbf{p}_1-\mathbf{b}_1 & \Re(\mathbf{p}_2-\mathbf{p}_1)-(\mathbf{b}_2-\mathbf{b}_1) & \Re(\mathbf{p}_3-\mathbf{p}_1)-(\mathbf{b}_3-\mathbf{b}_1) \\ \mathbf{b}_1\times(\mathbf{t}+\Re\mathbf{p}_1) & (\mathbf{b}_2-\mathbf{b}_1)\times\mathbf{t}+\mathbf{b}_2\times\Re\mathbf{p}_2 & (\mathbf{b}_3-\mathbf{b}_1)\times\mathbf{t}\mathbf{b}_3\times\Re\mathbf{p}_3 \\ & -\mathbf{b}_1\times\Re\mathbf{p}_1 & -\mathbf{b}_1\times\Re\mathbf{p}_1 \\ \mathbf{k}_1 & \mathbf{k}_2 & \mathbf{k}_3 \\ \mathbf{b}_1\times\mathbf{k}_1 & \mathbf{b}_2\times\mathbf{k}_2 & \mathbf{b}_3\times\mathbf{k}_3 \end{bmatrix}$$

[5]In this case, the leg vector $\mathbf{s}$ is $\mathbf{t}+\Re\mathbf{p}-\mathbf{b}$

Denoting the terms of the matrix which are linear functions of $\mathbf{X}$ (output position coordinates) as x^1 and all other constant terms as c for a fixed output orientation of the platform (i.e. $\Re$ is constant), the final matrix can be written in the form

$$\mathbf{H} \sim \begin{bmatrix} x^1 & c & c & c & c & c \\ x^1 & c & c & c & c & c \\ x^1 & c & c & c & c & c \\ x^1 & x^1 & x^1 & c & c & c \\ x^1 & x^1 & x^1 & c & c & c \\ x^1 & x^1 & x^1 & c & c & c \end{bmatrix}$$

On expanding the expression det $\mathbf{H} = 0$, we can see that maximum power of $\mathbf{X}$ appearing in the expression will be 3 and hence, for constant orientation of the output platform, the singularity manifold will be a hyper-surface of degree 3. The singularity curves along with the workspace boundaries(at different sections along Z-axis) are shown in the left column of figure 7. The workspace boundary has been evaluated based on the joint limits of all the 6 prismatic joints.

The controllability matrix for this manipulator has dimension 12×12. The regions where the STLC condition is violated along with the workspace boundary are shown on the right hand side of figure 7. It can be seen that the non-STLC regions are surrounding the singular zones.

4.3 Parallel manipulator with redundancy

If an additional actuated leg is added to the three-degree-of-freedom planar manipulator shown in figure 1, then we have the case of a redundant parallel manipulator with $m > n$.

The equations of motion for the planar redundant manipulator shown in figure 2 are

$$\mathbf{M} \begin{bmatrix} \ddot{\mathbf{t}} \\ \alpha \end{bmatrix} + \boldsymbol{\eta} = \mathbf{H}F \tag{14}$$

where the block elements of the mass matrix $\mathbf{M}$ are

$$\begin{aligned} \mathbf{M}_{11} &= M_p \mathbf{E}_2 + \sum_{i=1}^{4} \mathbf{Q}_i \\ \mathbf{M}_{12} &= {\mathbf{M}_{21}}^T = -(M_p \mathbf{R}_\perp + \sum_{i=1}^{4} \mathbf{Q}_i \mathbf{q}_{i\perp}) \\ \mathbf{M}_{22} &= I_p + M_p(R^2 \mathbf{E}_2 - \mathbf{R}\mathbf{R}^T) + \sum_{i=1}^{4} \mathbf{q}_{i\perp}^T \mathbf{Q}_i \mathbf{q}_{i\perp} \end{aligned}$$

and

$$\begin{aligned} \boldsymbol{\eta} &= \begin{bmatrix} M_p\{-\omega^2 \mathbf{R} - \mathbf{g}\} + \sum_{i=1}^{4} \mathbf{U}_i \\ -M_p \mathbf{R} \times \mathbf{g} + \sum_{i=1}^{4} \mathbf{q}_i \times \mathbf{U}_i \end{bmatrix} \\ \mathbf{H} &= \begin{bmatrix} \mathbf{s}_1 & \mathbf{s}_2 & \mathbf{s}_3 & \mathbf{s}_4 \\ \mathbf{q}_1 \times \mathbf{s}_1 & \mathbf{q}_2 \times \mathbf{s}_2 & \mathbf{q}_3 \times \mathbf{s}_3 & \mathbf{q}_4 \times \mathbf{s}_4 \end{bmatrix} \\ \mathbf{f} &= \begin{bmatrix} f_1 & f_2 & f_3 & f_4 \end{bmatrix}^T \end{aligned}$$

In the above equation, $\boldsymbol{\eta}$ is the column vector containing the centripetal, Coriolis and other non-linear terms, $\mathbf{H}$ is the force transformation matrix and vector $\mathbf{f}$ denotes the input actuations. The quantities, $\mathbf{Q}$, $\mathbf{U}$ and a_1 have the same meaning as in the previous manipulator.

In this case, the force transformation matrix is rectangular and of size (3×4) . To check the rank deficiency condition, 2 independent conditions are obtained by considering 2 separate combinations of 3 columns of the $\mathbf{H}$ matrix. It has been shown earlier that for a constant orientation of the output platform, the singularity curves will be quadratic in nature. Hence, the singularities of this redundant manipulator will be the points of intersection of these set of curves and with the help of Bezout's theorem we can conclude that there can be at most 4 singular points. Numerical simulation for this mechanism were done for the parameters listed in Appendix 1 and results obtained for constant orientation of the output platform.

Figure 6 shows the points (marked by *) where the redundant manipulator is singular. Comparing with figure 5, it is clear that the singular regions are greatly reduced by addition of an actuated leg. The uncontrollable regions for this manipulator are shown on the right-hand side of figure 6. It can be observed that, similar to the singular region, the non-STLC region is also greatly reduced by addition of an actuated leg.

For the case of the 3-PRPS hybrid manipulator, if we consider the redundant version with 2 extra actuators in an additional leg, we can observe that the singular and non-STLC regions are greatly reduced. This can be seen by comparing figures 7 and 8. In this case the force transformation matrix will be of size (6×8) and the singular regions will be the intersections of 2 hyper-surfaces of order 3. Numerical simulation for this mechanism were done for the parameters listed in Appendix 1 and results obtained for constant orientation of the output platform and at particular sections in Z-direction are shown in figure 8.

4.4 Manipulator with $m < n$

The 3-RPS spatial manipulator shown in figure 3 has six output variables (3 position co-ordinates and 3 orientation co-ordinates for the moving platform) and it has three degrees of freedom with three actuated prismatic joints. All the other revolute and spherical joints are passive. In this manipulator, the six output variables are not independent.

The equations of motion for the 3-RPS manipulator are six second-order differential equations and three algebraic constraints. These are given as

$$\mathbf{M} \begin{bmatrix} \ddot{\mathbf{t}} \\ \boldsymbol{\alpha} \end{bmatrix} + \boldsymbol{\eta} = \mathbf{H}_s \mathbf{F} + \mathbf{H}_k \boldsymbol{\lambda} \tag{15}$$

$$\mathbf{S}_i \cdot \mathbf{k}_i = 0 \qquad \text{for } i \ = 1 \text{ to } 3 \tag{16}$$

where the block elements of the mass matrix $\mathbf{M}$ are

$$\begin{aligned}
\mathbf{M}_{11} &= M_p\mathbf{E}_3 + \sum_{i=}^{3}\mathbf{Q}_i \\
\mathbf{M}_{12} &= -\mathbf{M}_{21} = -M_p\tilde{\mathbf{R}} - \sum_{i=1}^{3}\mathbf{Q}_i\tilde{\mathbf{q}}_i \\
\mathbf{M}_{22} &= \mathbf{I}_p + M_p(\mathbf{R}^2\mathbf{E}_3 - \mathbf{R}\mathbf{R}^T) + \sum_{i=1}^{3}\tilde{\mathbf{q}}_i\mathbf{Q}_i\tilde{\mathbf{q}}_i
\end{aligned}$$

and

$$\begin{aligned}
\boldsymbol{\eta} &= \begin{bmatrix} M_p\{\boldsymbol{\omega}\times(\boldsymbol{\omega}\times\mathbf{R}) - \mathbf{g}\} + \sum_{i=1}^{3}\mathbf{U}_i \\ \boldsymbol{\omega}\times(\mathbf{I}_p\boldsymbol{\omega}) + M_p\mathbf{R}\times\{(\boldsymbol{\omega}\cdot\mathbf{R})\boldsymbol{\omega} - \mathbf{g}\} + \sum_{i=1}^{3}\mathbf{q}_i\times\mathbf{U}_i \end{bmatrix} \\
\mathbf{H}_s &= \begin{bmatrix} \mathbf{s}_1 & \mathbf{s}_2 & \mathbf{s}_3 \\ \mathbf{q}_1\times\mathbf{s}_1 & \mathbf{q}_2\times\mathbf{s}_2 & \mathbf{q}_3\times\mathbf{s}_3 \end{bmatrix} \\
\mathbf{H}_k &= \begin{bmatrix} \mathbf{k}_1 & \mathbf{k}_2 & \mathbf{k}_3 \\ \mathbf{q}_1\times\mathbf{k}_1 & \mathbf{q}_2\times\mathbf{k}_2 & \mathbf{q}_3\times\mathbf{k}_3 \end{bmatrix}
\end{aligned}$$

$$\mathbf{F} = \begin{bmatrix} F_1 & F_2 & F_3 \end{bmatrix}^T \qquad \text{and} \qquad \boldsymbol{\lambda} = \begin{bmatrix} \lambda_1 & \lambda_2 & \lambda_3 \end{bmatrix}^T$$

The constraint equations $\mathbf{S}_i\cdot\mathbf{k}_i = 0, \quad i = 1,2,3$, express the condition that the direction of the i-th leg ($\mathbf{s}$) is always orthogonal to that of the revolute axis $\mathbf{k}$. As before, $\boldsymbol{\eta}$ contains all the centripetal and Coriolis terms, the rectangular matrices $\mathbf{H}_s$ and $\mathbf{H}_k$ form the force transformation matrix $\mathbf{H}$, $\mathbf{F}$ denote the input actuations, $\boldsymbol{\lambda}$ correspond to the Lagrange multipliers, $\mathbf{k}_i$ signifies the direction of the revolute joint axes at the base, $\mathbf{s}_i$ is the unit vector along the $i-$th leg and ($\tilde{}$) denotes the skew-symmetric matrix.

The terms a_1, $\mathbf{Q}$ and $\mathbf{U}$ are given as

$$\begin{aligned}
&a_1 = m_d(\mathbf{k}\times\mathbf{r}_d)^2 + m_u(\mathbf{k}\times\mathbf{r}_u)^2 + (\mathbf{I}_u + \mathbf{I}_d) \\
&\mathbf{Q} = m_u\mathbf{s}\mathbf{s}^T + \tfrac{m_u}{L_2}(\mathbf{s}\cdot(\mathbf{k}\times\mathbf{r}_u))(\mathbf{s}(\mathbf{k}\times\mathbf{s})^T + (\mathbf{k}\times\mathbf{s})\mathbf{s}^T + a_1(\mathbf{k}\times\mathbf{s})(\mathbf{k}\times\mathbf{s})^T \\
&\mathbf{U} = [m_u(\mathbf{s}\cdot\mathbf{g}) - m_u\mathbf{s}\cdot(\mathbf{W}\cdot(\mathbf{W}\times\mathbf{r}_u)) - m_u\mathbf{s}\cdot\mathbf{u}_3 \\
&-\tfrac{m_u}{L}\{\mathbf{s}\cdot(\mathbf{k}\times\mathbf{r}_u)\}\{(\mathbf{k}\times\mathbf{s})\cdot\mathbf{u}_4\}]\mathbf{s} \\
&+[m_u\mathbf{k}\cdot(\mathbf{r}_u\times\mathbf{g}) + m_d\mathbf{k}\cdot(\mathbf{r}_d\times\mathbf{g}) - \mathbf{k}\cdot\{\mathbf{W}\times(\mathbf{I}_u + \mathbf{I}_d)\mathbf{W}\} - a_1\mathbf{u}_4 \\
&-m_u\mathbf{k}\cdot(\mathbf{r}_u\times\mathbf{s})\mathbf{u}_3](\mathbf{k}\times\mathbf{s})
\end{aligned}$$

The force transformation matrix is obtained by considering the effect of both the actuated and constraint forces. The matrix, $\mathbf{H}_s$, corresponding to actuations are obtained from the Plücker coordinates of the legs and the matrix, $\mathbf{H}_k$, due to the constraint forces are the Plücker coordinates of the revolute axes. The manipulator reaches singular configurations when either the matrix $\mathbf{H}_s$ or $\mathbf{H}_k$ or the entire matrix $\mathbf{H}$ loses rank and these result in the actuation

or constraint forces becoming infinite or the manipulator is being unable to resist a certain combination of external forces and moments with actuator and constraint forces. When the rank of $\mathbf{H}_s$ is less than 3, the mechanism is unable to withstand 4 out of the 6 externally applied forces. At these configurations, the legs are either parallel or concurrent. When legs are parallel, the manipulator will not be able to resist external forces and when the legs are concurrent, the manipulator will not be able to resist external moments.

Numerical simulation results based on the mechanism parameters given in Appendix 1 are shown in figure 9 where we plot the singular and uncontrollable regions on the left and right-hand side respectively. The workspace boundary is calculated based on the leg-length limits satisfying the constraint equations. The non-STLC regions along with the positions at which the Lagrange multipliers become infinite(marked by *) are shown in the right hand column. It can be observed that the Lagrange multipliers become infinite at some of the regions where the system does not meet the STLC requirement.

4.5 Manipulator with $m < DOF$

If we use 2 actuators for the 3-DOF manipulator as shown in figure 1, then the manipulator is under-actuated. For this specific case the $\mathbf{H}$ matrix will be rectangular of dimension 3×2. The manipulator will encounter force singularities when the rank of $\mathbf{H}$ matrix becomes less than 2. The numerical simulation for case is shown in figure 10. The singular and non-STLC regions are shown side by side. The numerical results were obtained by not actuating one of the legs in the 3-DOF manipulator shown in figure 1.

5 Conclusion

In this paper, we have analyzed the singularities and uncontrollable regions in parallel manipulators and closed-loop mechanisms. The singularities associated with a gain of degree of freedom were obtained by considering the rank deficiency of the force transformation matrix. The uncontrollable regions of a parallel manipulator or a closed loop mechanism were obtained by considering the rank deficiency of the controllability matrix after deriving the equations of motion in terms of Cartesian space variables. The parallel manipulators and closed-loop mechanisms are classified according to their degrees of freedom, the number of output Cartesian variables used to describe their motion and the number of actuated joint inputs. In all the cases, we have showed that the singular regions are a subset of the uncontrollable regions. In some cases, parallel manipulators and closed-loop mechanisms can also become uncontrollable when the Lagrange multipliers representing constraint forces/torques at the passive joints become infinite. Adding a redundant actuator is shown to reduce singular and uncontrollable

regions in parallel manipulators and closed-loop mechanisms. The above results have been illustrated with the help of several planar and spatial manipulators and closed-loop mechanisms.

6 Acknowledgment

The authors wish to thank Bhaskar Dasgupta and Rex J. Theodore for their valuable suggestions and comments.

References

[Basu and Ghosal, 1997] Basu, D., and Ghosal, A., 'Singularity Analysis of Platform Type Multi-Loop Spatial Mechanism', *Mechanism and Machine Theory*, Vol. 32, No. 3, pp. 375-389, 1997.

[Behi, 1988] Behi, H., 'Kinematic Analysis of a 6-DOF 3-PRPS Parallel Mechanism' *IEEE Trans. on Robotics and Automation*, Vol. 4, No. 5, pp. 561-565, 1988.

[Bloch and McClamroch, 1990] Bloch, A. M., and McClamroch, N.H., 'Controllability and Stabilizibility Properties of a Nonholonomic Control System', *Proc. IEEE Conf. on Decision Control*, pp. 1312-1314, 1990.

[Chang and Khatib, 1995] Chang, K., and Khatib, O., 'Manipulator Control at Kinematic Singularities: A Dynamically Consistent Strategy',*Proc. IEEE Conf. on Intelligent Robot Systems*, pp. 84-88, 1995.

[Chevallereau, 1996] Chevallereau, C., 'Feasible trajectories for non redundant robot at a singularity', *Proc. of IEEE Conf. on Robotics and Automation*, pp. 1871-1876, 1996.

[Choudhury, 1997] Choudhury, P., 'Dynamics, Singularity and Controllability Analysis of Closed-Loop Manipulators', *Master's Thesis, Indian Institute of Science, Bangalore*, 1997.

[Collins and Long, 1995] Collins, C. L., and Long, C. L., 'The Singularity Analysis of an In-Parallel Hand Controller for Force-Reflected Teleoperation', *IEEE Transactions on Robotics and Automation*, Vol. 11, No. 5, pp. 661-669, 1995.

[Danielli et. al, 1995] Danielli, H. R. M., Zsombor-Murray, P. J., and Angeles, J., 'Singularity Analysis of Planar Parallel Manipulators', *Mechanism and Machine Theory*, Vol. 30, No. 5, pp. 665-678, 1995.

[Dasgupta and Mruthyunjaya, 1998] Dasgupta, B., and Mruthyunjaya, T. S., 'Force Redundancy in Parallel Manipulators: Theoretical and Practical Issues', *Mechanism and Machine Theory* (to appear), 1998.

[Fichter, 1986] Fichter, E. F., 'A Stewart Platform-Based Manipulator: General Theory and Practical Construction', *Int. Journal of Robotics Research*, Vol. 5, No. 2, pp. 157-182, 1986.

[Gosselin and Angeles, 1990] Gosselin, C., and Angeles, J., 'Singularity Analysis of Closed-Loop Kinematic Chains', *IEEE Trans. on Robotics and Automation*, Vol. 6, No. 3, pp. 281-290, 1990.

[Herman and Krenner, 1977] Hermann, R., and Krenner, A. J., 'Non-Linear Controllability and Observability', *IEEE Transactions on Automatic Control*, Vol. AC22, pp. 728-740, 1977.

[Hunt, 1978] Hunt,K. H., *Kinematic Geometry of Mechanisms*, Clarendon Press, Oxford, 1978.

[Hunt, 1986] Hunt, K. H., 'Special configurations of robot arms via screw theory, Part 1. The Jacobian and its matrix cofactors', *Robotica*, Vol. 4, pp. 171-179, 1986.

[Isidori, 1995] Isidori, A., *Non-Linear Control Systems*, Springer Verlag, 1995.

[Krishnan and McClamroch, 1994] Krishnan, H., and McClamroch, N. H., 'Tracking in Nonlinear Differential-Algebraic Control Systems with Application to Constrained Robot Systems', *Automatica*, Vol. 30, No. 2, pp. 1885-1897, 1994.

[Karger, 1996] Karger, A., 'Singularity analysis of serial-robot manipulators', *Trans. of ASME, Journal of Mechanical Design*, Vol. 118, pp. 520-525, 1996.

[Lipkin and Pohl, 1991] Lipkin, H., and Pohl, E., 'Enumeration of singular configurations for robotic manipulators', *Trans. of ASME, Journal of Mechanical Design*, Vol. 113, pp. 272-279, 1991.

[Lloyd, 1996] Lloyd, J. E., 'Using puiseux series to control non-redundant robots at singularities', *Proc. of IEEE Conf. on Robotics and Automation*, pp. 1877-1882, 1996.

[Merlet, 1989] Merlet, J. P., 'Singular Configurations of Parallel Manipulators and Grassman Geometry', *Int. Journal of Robotics Research*, Vol. 8, No. 5, pp. 45-56, 1989.

[Nijmeijer, 1990] Nijmeijer, H., and van der Schaft, J. A., *Nonlinear Dynamical Control Systems*, Springer Verlag, 1990.

[Sarkar et. al., 1994] Sarkar, N.,Yun, X., and Kumar, V., 'Control of Mechanical Systems With Rolling Constraints: Application to Dynamic Control of Mobile Robots', *Int. Journal of Robotics Research*, Vol. 13, No. 1, pp. 55-69, 1994.

[Sefrioui and Gosselin, 1995] Sefrioui, J., and Gosselin, C., 'On the Quadratic Nature of the Singularity Curves of Planar Three-Degree-of-Freedom Parallel Manipulators', *Mechanism and Machine Theory*, Vol. 30, No. 4, pp. 533-551, 1995.

[Shamir, 1990] Shamir, T., 'The singularities of redundant robot arms', *International Journal of Robotics Research*, Vol. 9, No. 1, pp. 113-121, 1990.

[Spong and Vidyasagar, 1989] Spong, M. W., and Vidyasagar, M., *Robot Dynamics and Control*, John Wiley and Sons, 1989.

[Sussman and Jurdjevic, 1972] Sussman, H. J., and Jurdjevic, V., 'Controllability of Non-Linear Systems', *Journal of Differential Equations*, Vol. 12, pp. 95-116, 1972.

[Sugimoto et. al., 1982] Sugimoto, K., Duffy, J., and Hunt, K. H. , 'Special configurations of spatial mechanisms and robot arms', *Mechanisms and Machine Theory*, Vol. 17, pp. 119-132, 1982.

[Tchnon and Matuszok, 1995] Tchnon, K., and Matuszok, A., 'On avoiding singularity in redundant robot kinematics', *Robotica*, Vol. 13, pp. 599-606, 1995.

[Wang and Waldron, 1987] Wang, S. L., and Waldron, K. J., 'A study of the singular configurations of serial manipulators', *Trans. of ASME, Journal of Mechanism, Transmissions and Automation in Design*, Vol. 109, pp.14-20, 1987.

[Zlatanov et. al., 1995] Zlatanov, D., Fenton, R. G., and Benhabib, B., 'A Unifying Framework for Classifying and Interpretation of Mechanism Singularities', *Trans. ASME, Journal Mechanical Design*, Vol. 117, pp. 566-572, 1995.

Appendix 1

All the numerical values given in this Appendix are in SI-units.

3-DOF Planar Manipulator with Prismatic Actuations

Leg length limits for each leg : 0.2 to 1.0

Co-ordinates of base and platform points(in local frame), centres of gravity of lower and upper

parts of each leg(in local frame) and centre of gravity of the platform(in local frame) are given by

$\mathbf{b}_1$	$\mathbf{b}_2$	$\mathbf{b}_3$	$\mathbf{p}_1$	$\mathbf{p}_2$	$\mathbf{p}_3$	$\mathbf{r}_{d0}$	$\mathbf{r}_{u0}$	$\mathbf{R}_0$
0.0	0.2	0.4	-0.15	-0.1	0.15	0.1	-0.15	0.04
0.0	0.0	0.1	0.0	-0.1	0.0	0.0	0.0	0.005

Mass and moments of inertia(about base joint) of lower and upper part of each leg and that of the platform are

m_d	m_u	I_d	I_u	M_p	I_p
0.6	0.2	0.01	0.008	2.0	0.075

3-DOF Redundant Manipulator

The co-ordinates of the base and platform points(in local frame) are listed below:

$\mathbf{b}_1$	$\mathbf{b}_2$	$\mathbf{b}_3$	$\mathbf{b}_4$	$\mathbf{p}_1$	$\mathbf{p}_2$	$\mathbf{p}_3$	$\mathbf{p}_4$
0.0	0.2	0.4	0.2	-0.15	-0.1	0.15	-0.1
0.0	0.0	0.1	0.2	0.0	-0.1	0.0	0.15

All other parameters are similar to the above section 6.

3-PRPS Hybrid Manipulator

Leg length limits for bottom leg with prismatic joint: 0.65 to 0.3
Leg length limits for upper leg with prismatic joint: 0.65 to 1.75
Co-ordinates of base and platform points(in local frame), centres of gravity of lower, middle and upper parts of each leg(in local frame) and centre of gravity of the platform(in local frame) are given by

$\mathbf{b}_1$	$\mathbf{b}_2$	$\mathbf{b}_3$	$\mathbf{p}_1$	$\mathbf{p}_2$	$\mathbf{p}_3$	$\mathbf{r}_{d0}$	$\mathbf{r}_{m0}$	$\mathbf{r}_{u0}$	$\mathbf{R}_0$
0.4	0.1	-0.3	0.2	0.2	0.0	0.4	0.14	-0.18	0.04
0.2	0.2	0.15	0.0	0.15	0.2	0.6	-0.08	0.08	0.03
0.0	0.1	0.1	0.1	0.0	0.0	0.0	0.0	0.0	-0.06

The direction of the fixed axis along the lower prismatic joint is given by:

$\mathbf{k}_1$	$\mathbf{k}_2$	$\mathbf{k}_3$
-0.6141	0.2308	0.5535
0.2714	0.4231	0.2860
0.0000	0.0077	0.0953

Mass of lower, middle and upper part of each leg and that of the platform are

m_d	m_m	m_u	M_p
3.0	2.0	1.0	6.0

Moments of inertia of lower, middle and upper part of the leg (in local frame) are given by:

$$\mathbf{I}_{d0} = \begin{bmatrix} 0.004 & 0.001 & 0.002 \\ 0.001 & 0.002 & 0.001 \\ 0.001 & 0.001 & 0.002 \end{bmatrix} \quad \text{and} \quad \mathbf{I}_{m0} = \begin{bmatrix} 0.010 & 0.005 & 0.007 \\ 0.005 & 0.002 & 0.003 \\ 0.007 & 0.003 & 0.001 \end{bmatrix} \mathbf{I}_{u0} = \begin{bmatrix} 0.005 & 0.002 & 0.002 \\ 0.002 & 0.002 & 0.001 \\ 0.002 & 0.001 & 0.002 \end{bmatrix}$$

The moment of inertia of platform (in local frame) is given as

$$\mathbf{I}_p = \begin{bmatrix} 0.02 & 0.001 & 0.003 \\ 0.001 & 0.020 & 0.002 \\ 0.002 & 0.002 & 0.050 \end{bmatrix}$$

3-PRPS Redundant Manipulator

The co-ordinates of the base and platform points(in local frame) are listed below:

$\mathbf{b}_1$	$\mathbf{b}_2$	$\mathbf{b}_3$	$\mathbf{b}_4$	$\mathbf{p}_1$	$\mathbf{p}_2$	$\mathbf{p}_3$	$\mathbf{p}_4$
0.4	0.1	-0.3	0.05	0.2	0.2	0.0	0.1
0.2	0.2	0.15	0.25	0.0	0.15	0.2	0.25
0.0	0.1	0.1	0.05	0.1	0.0	0.0	0.05

All other parameters are similar to the above section 6.

3-RPS Manipulator

The leg lengths are taken to vary between 0.2 to 0.65. Co-ordinates of base and platform points(in local frame), direction of the revolute axes and centres of gravity of lower and upper parts and platform(in local frame) are:

$\mathbf{b}_1$	$\mathbf{b}_2$	$\mathbf{b}_3$	$\mathbf{p}_1$	$\mathbf{p}_2$	$\mathbf{p}_3$	$\mathbf{k}_1$	$\mathbf{k}_2$	$\mathbf{k}_3$
.1	.4	-.4	.1	.3	-.2	.4	-.7	.3
.2	.5	-.3	.1	.2	-.1	.1	-.1	.2
0	.01	.01	0	0	0	0	.0007	.0003

The vectors $\mathbf{r}_{d0}$, $\mathbf{r}_{u0}$, and $\mathbf{R}_0$ are given as $(0.2, 0, 0)^T$, $(-0.15, 0, 0)^T$, and $(0.003, 0.003, 0.003)^T$ respectively.

The masses of the lower, the upper part of each leg and the platform are 0.5, 0.2 and 0.4 Kg's respectively, and the moments of inertia of lower and upper parts of each leg (in the local frames) are given as

$$\mathbf{I}_{d0} = \begin{bmatrix} 0.010 & 0.005 & 0.007 \\ 0.005 & 0.002 & 0.003 \\ 0.007 & 0.003 & 0.001 \end{bmatrix} \quad \text{and} \quad \mathbf{I}_{d0} = \begin{bmatrix} 0.005 & 0.002 & 0.002 \\ 0.002 & 0.002 & 0.001 \\ 0.002 & 0.001 & 0.003 \end{bmatrix}$$

The moment of inertia of platform (in local frame) is given as

$$\mathbf{I}_p = \begin{bmatrix} 0.010 & 0.000 & 0.000 \\ 0.000 & 0.020 & 0.000 \\ 0.000 & 0.000 & 0.075 \end{bmatrix}$$

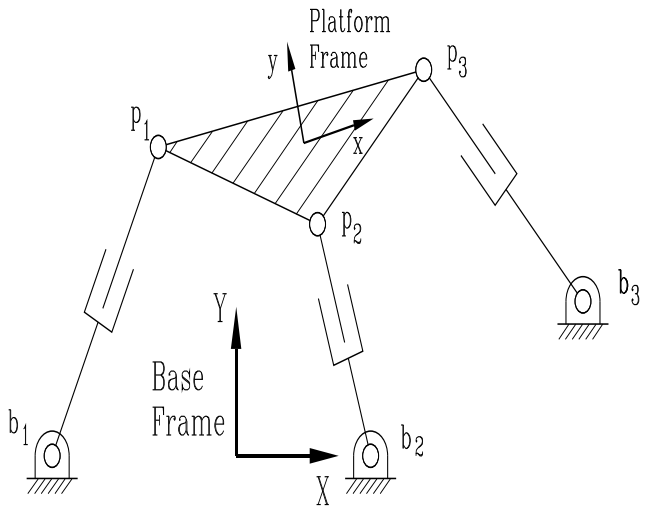

Figure 1: 3-DOF Planar Parallel Manipulator

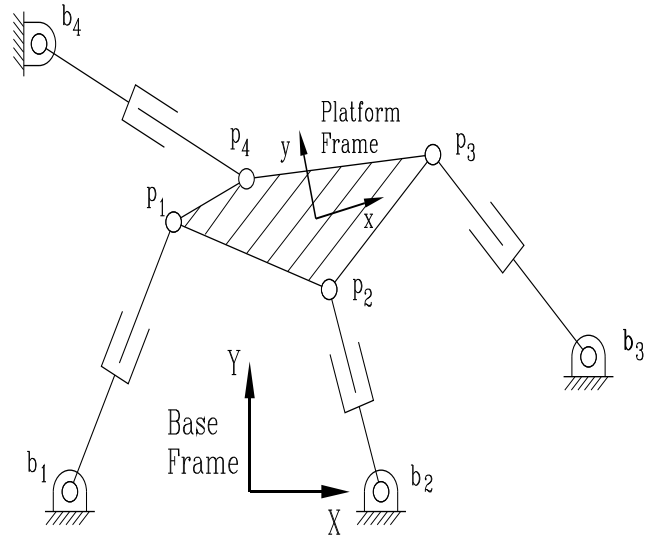

Figure 2: 3-DOF Planar Redundant Manipulator

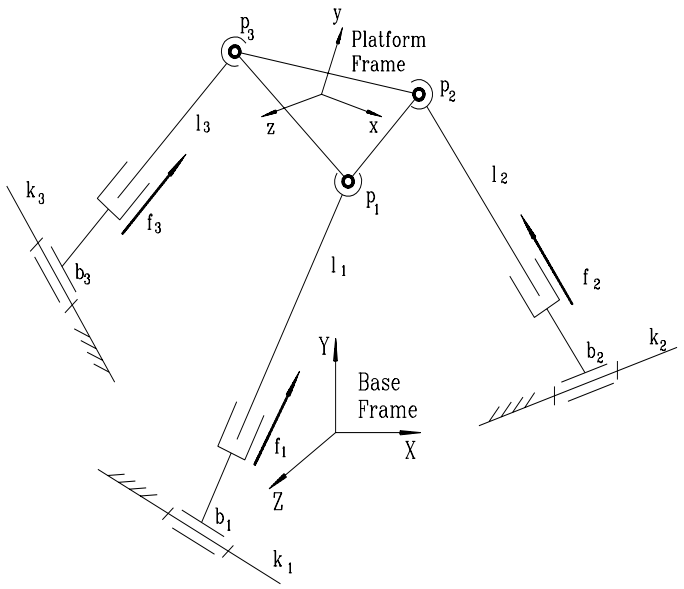

Figure 3: 3-RPS Spatial Manipulator

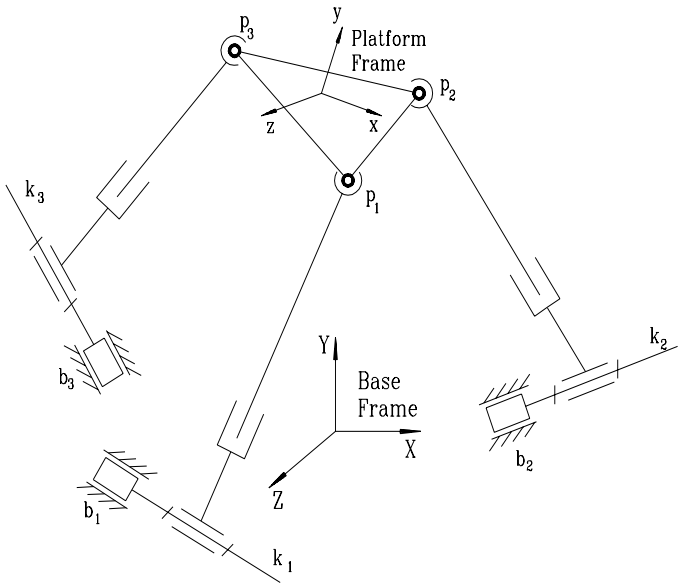

Figure 4: 3-PRPS Spatial Manipulator

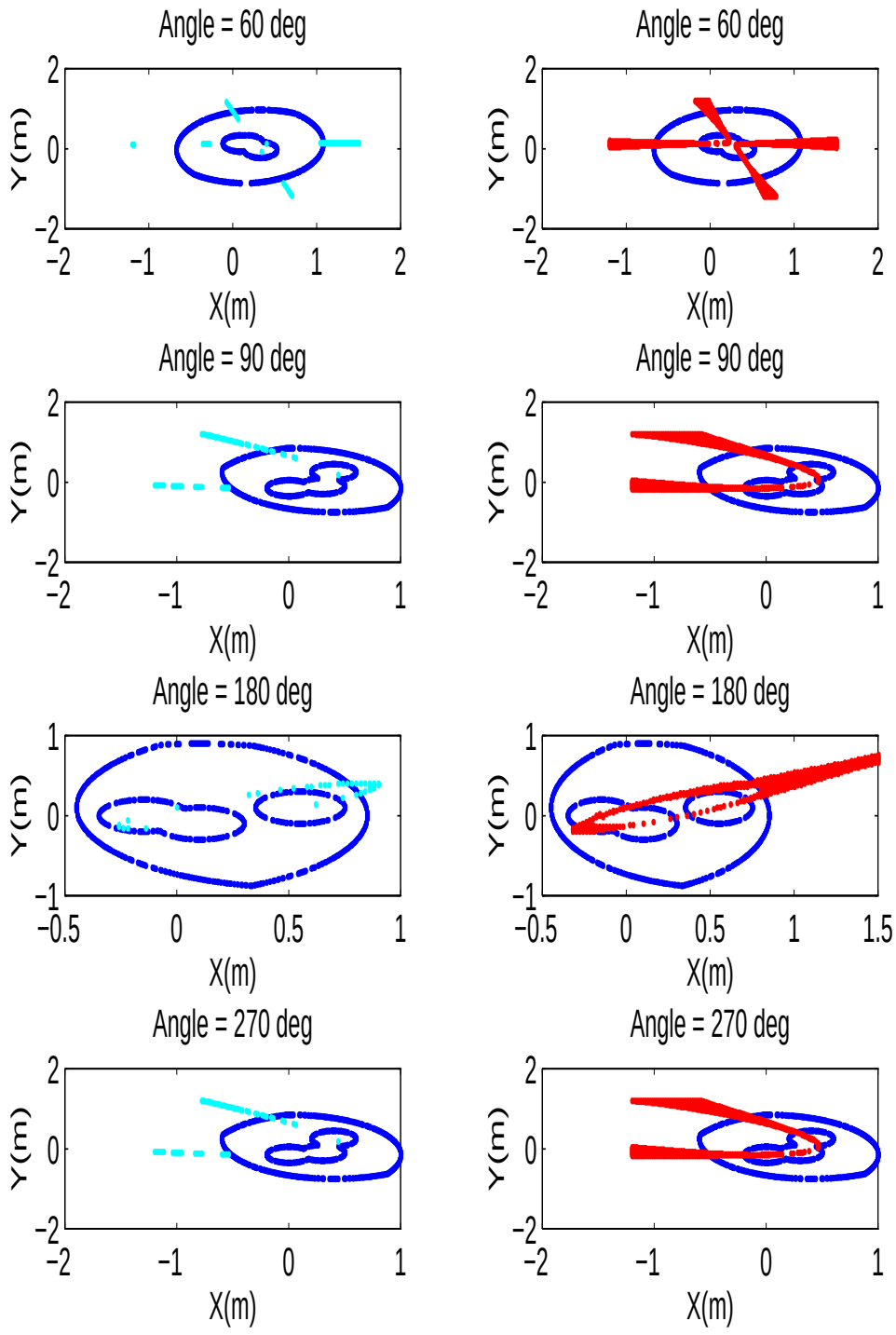

Figure 5: Singular and Uncontrollable Regions of a 3-DOF Planar Manipulator

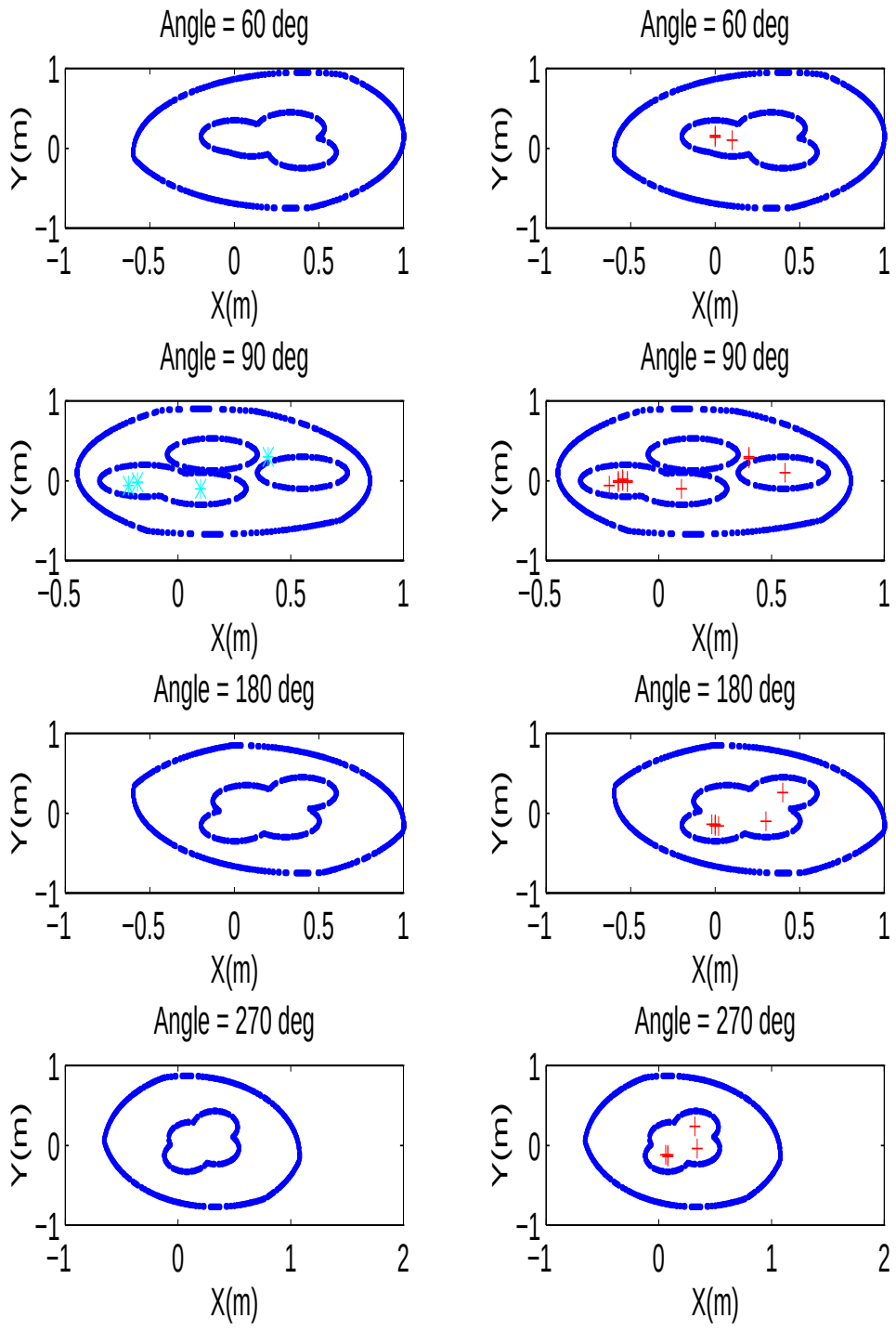

Figure 6: Singular and Uncontrollable Regions of a 3-DOF Planar Redundant Manipulator

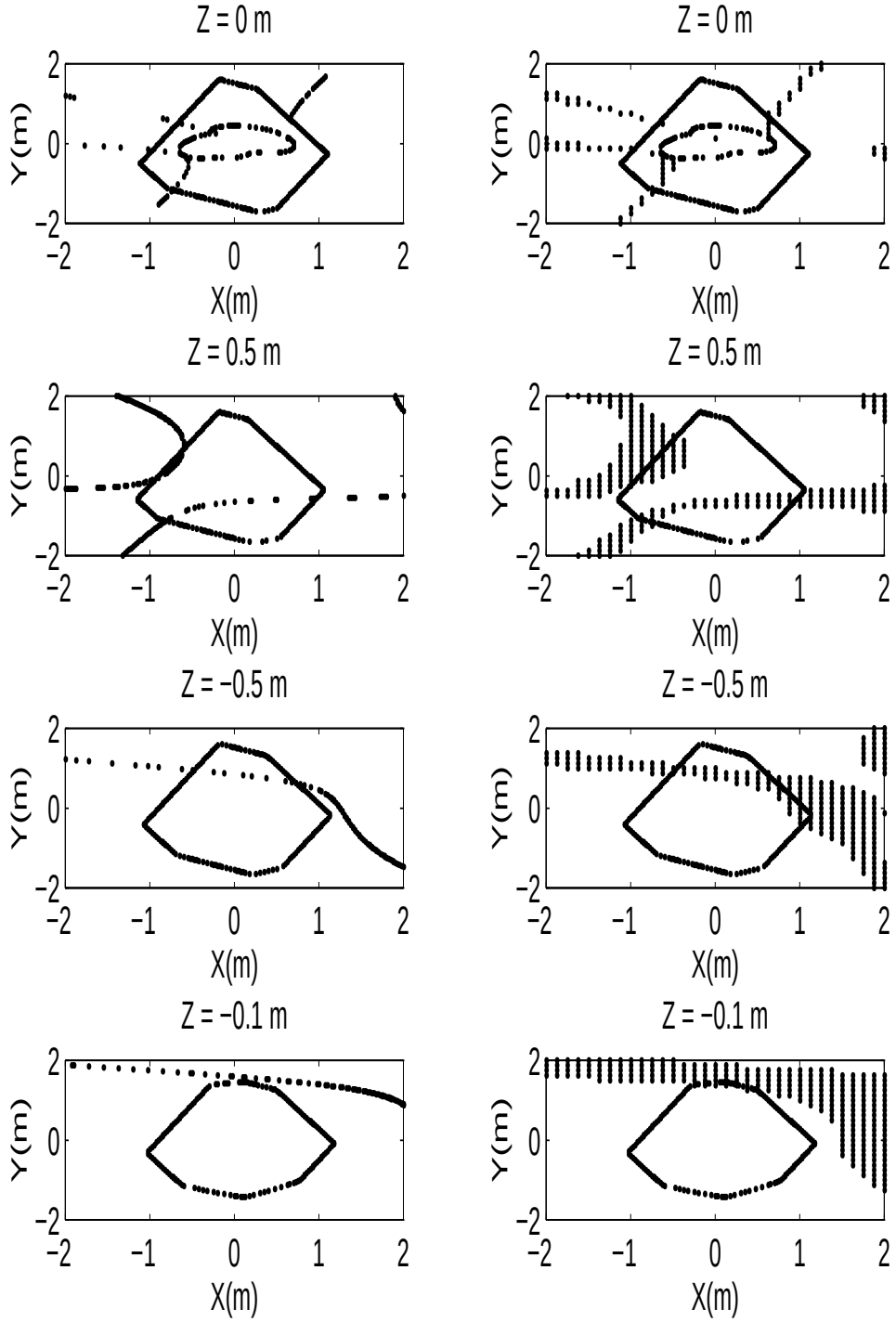

Figure 7: Singular and Uncontrollable Regions of a 3-PRPS Manipulator

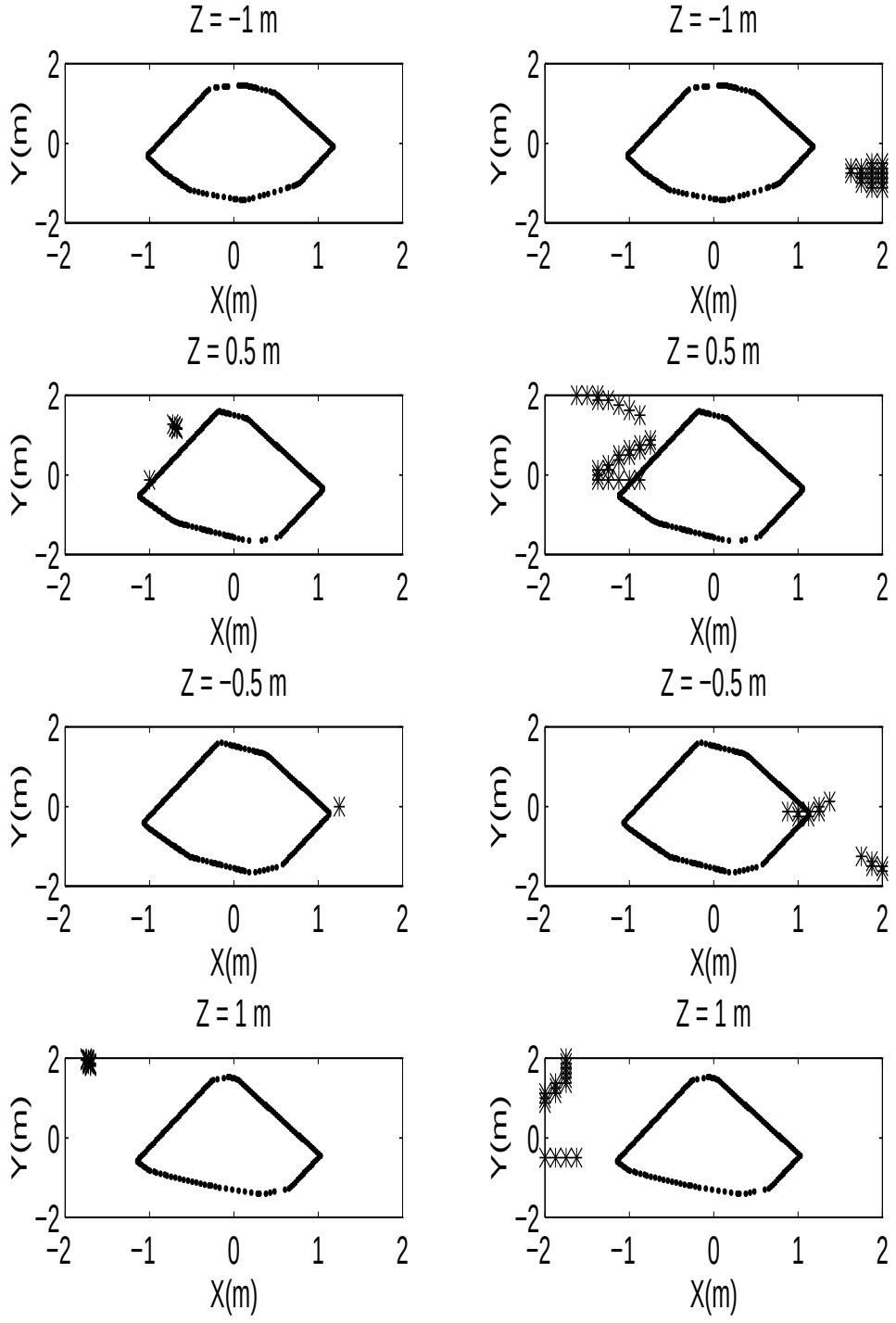

Figure 8: Singular and Uncontrollable Regions of a 3-PRPS Redundant Manipulator

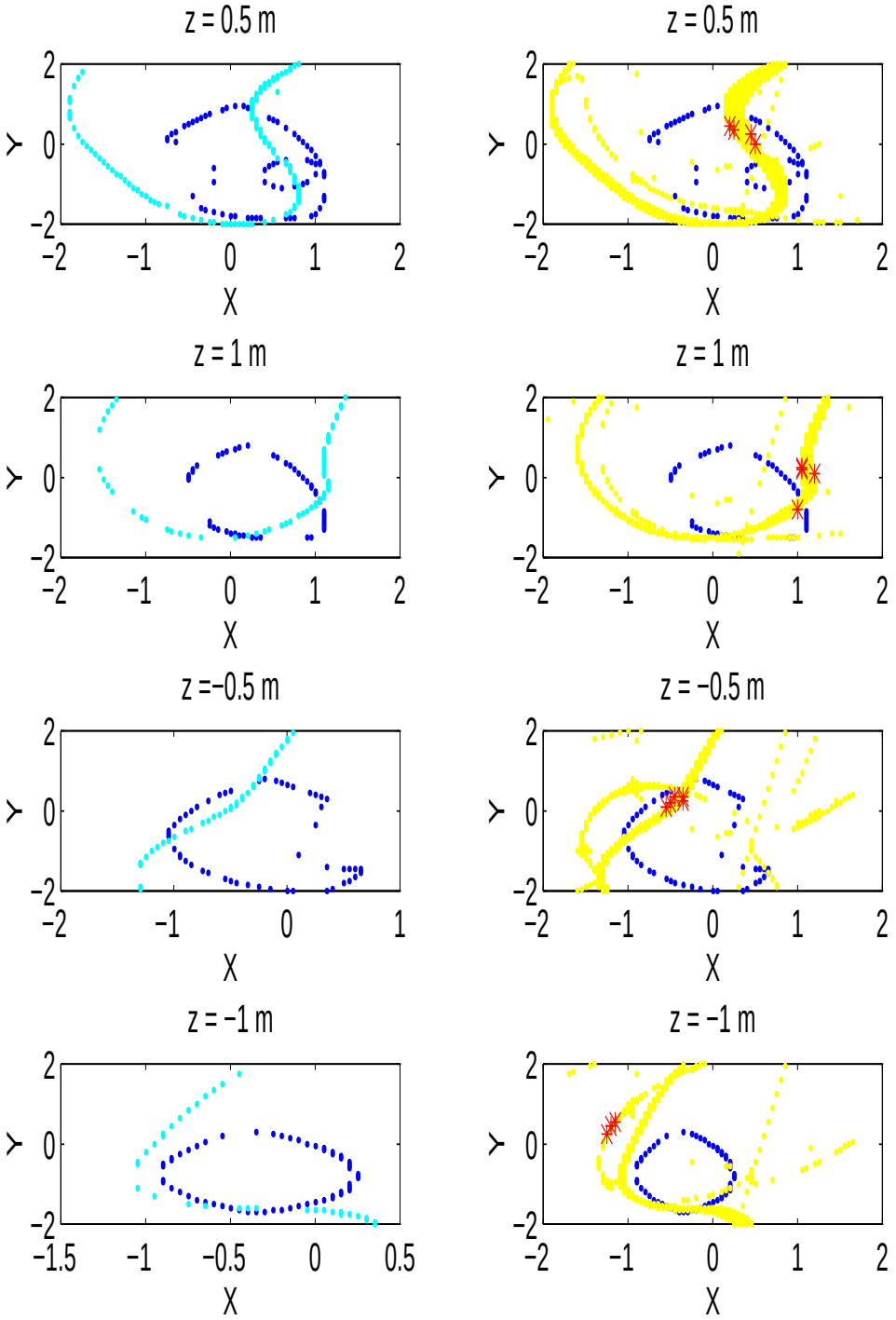

Figure 9: Singular and Uncontrollable Regions of a 3-DOF Spatial Manipulator

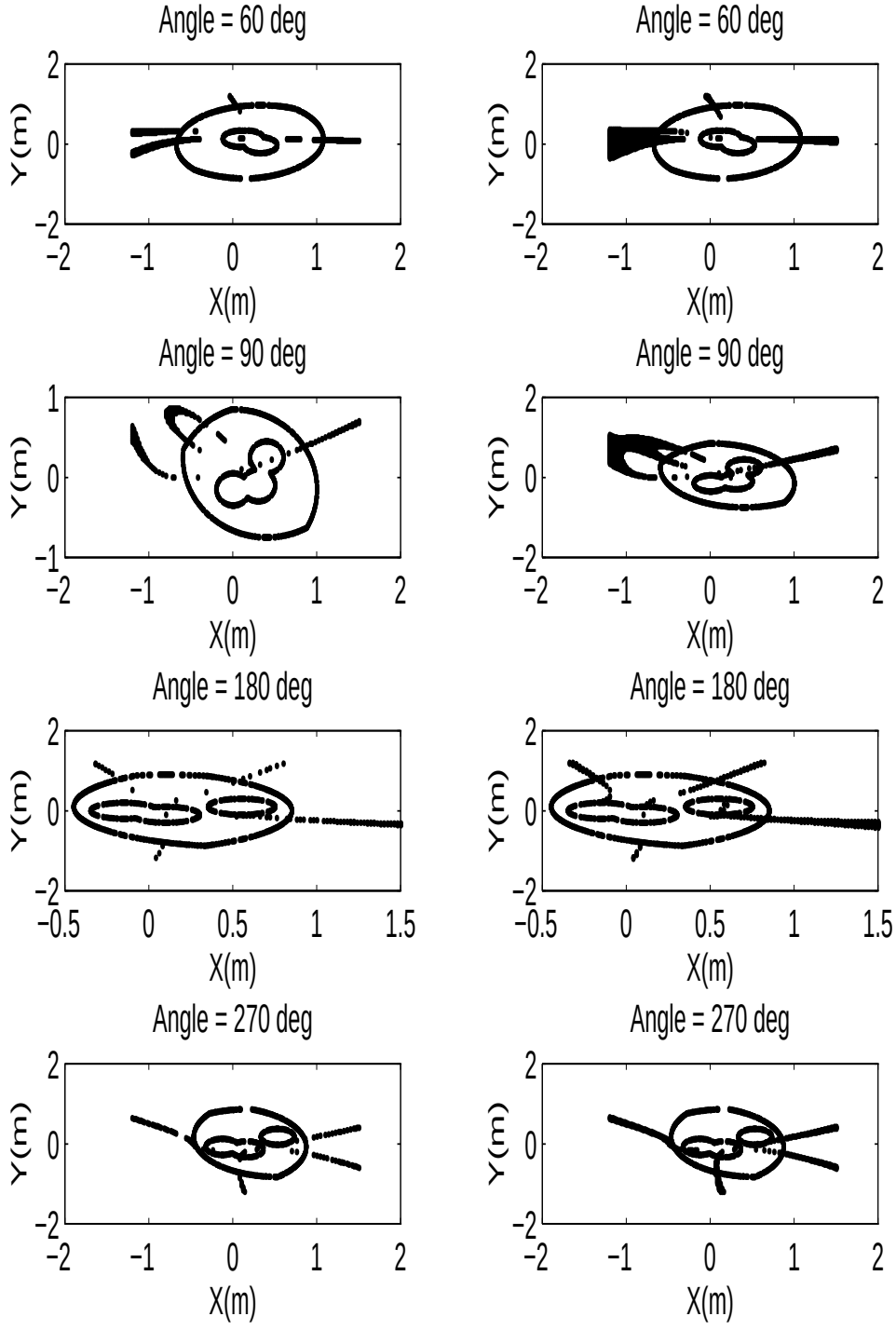

Figure 10: Singular and Uncontrollable Regions of an under-actuated Manipulator